Available online at www.sciencedirect.com
SCIENCE DIRECT®
APPLIED MATHEMATICS AND COMPUTATION
ELSEVIER Applied Mathematics and Computation 167 (2005) 435–453
www.elsevier.com/locate/amc

An efficient method to compute singularity induced bifurcations of decoupled parameter-dependent differential-algebraic power system model

Saffet Ayasun [a,*], Chika O. Nwankpa [b], Harry G. Kwatny [c]

[a] *Department of Electrical and Electronics Engineering, Nigde University, 51200, Nigde, Turkey*
[b] *Department of Electrical and Computer Engineering, Drexel University, 19104, Philadelphia, PA, USA*
[c] *Department of Mechanical Engineering and Mechanics, Drexel University, 19104, Philadelphia, PA, USA*

Abstract

In this paper, we present an efficient method to compute singular points and singularity induced bifurcation points of differential-algebraic equations (DAEs) for a multi-machine power system model. The algebraic part of the DAEs brings singularity issues into dynamic stability assessment of power systems. Roughly speaking, the singular points are points that satisfy the algebraic equations, but at which the vector field is not defined. In terms of power system dynamics, around singular points, the generator angles (the natural states variables) are not defined as a graph of the load bus variables (the algebraic variables). Thus, the causal requirement of the DAE model breaks down and it cannot predict system behavior. Singular points constitute important organizing

* Corresponding author.
E-mail addresses: saffet@nwankpa.ece.drexel.edu, sayasun@nigde.edu.tr (S. Ayasun), chika@nwankpa.ece.drexel.edu (C.O. Nwankpa), hkwatny@coe.drexel.edu (H.G. Kwatny).

0096-3003/$ - see front matter
doi:10.1016/j.amc.2004.07.011

elements of power system DAE models. This paper proposes an iterative method to compute singular points at any given parameter value. Generator angles are parameterized through a scalar parameter in the constraint manifold and identification of singular points is formulated as a bifurcation problem of the algebraic part of the DAEs. Singular points are determined using a second order Newton–Raphson method. Moreover, the decoupled structure of the DAE model is exploited to find new set of parameters and parameter increase pattern which will result in a set of equilibria including singularity induced bifurcations. The simulation results are presented for a 5-bus power system and singular and singularity induced bifurcation points are depicted together with equilibria to visualize static and dynamic stability limits.

Keywords: Differential-algebraic equation; Voltage stability; Constraint manifold; Singular point; Singularity induced bifurcation

1. Introduction

The differential-algebraic equations (DAEs) are widely used to describe the dynamics of many systems such non-linear electric circuits, multibody mechanical systems, chemical processes and electric power systems. The dynamics of a classical power system with constant PQ load buses are commonly described by semi-explicit differential-algebraic equation (DAE) of the form [1,2]:

$$\begin{aligned} &\dot{\delta}_{\mathrm{g}} = \omega, \\ &\dot{\omega} = -[M^{-1}D]\omega - M^{-1}[f_{\mathrm{g}}(\delta_{\mathrm{g}}, \delta_{\ell}, V) - P_{\mathrm{g}}], \\ &f_{\ell}(\delta_{\mathrm{g}}, \delta_{\ell}, V) - P_{\ell} = 0, \\ &g_{\ell}(\delta_{\mathrm{g}}, \delta_{\ell}, V) - Q_{\ell} = 0, \end{aligned} \tag{1}$$

where δ_{g} is the vector of generators' rotor angles, ω is the vector of generators' angular velocities, δ_{ℓ} is the vector of phase angles of voltages at the load buses, V is the vector of voltage magnitudes, M is the inertia matrix, D is the damping matrix, P_{g} is the vector of net real power injections at the generator buses, and finally P_{ℓ} and Q_{ℓ} are the vectors of net real and reactive power injections at the load buses, respectively. The differential equation is the swing equation describing dynamics of each generator, and algebraic equations are the power flow equations representing real and reactive power balances at the load buses. In order to obtain a compact form of (1), if we let $x = [\delta_{\mathrm{g}}^{\mathrm{T}}\ \omega^{\mathrm{T}}]^{\mathrm{T}}$, $y = \delta_{\ell}^{\mathrm{T}}\ V^{\mathrm{T}}]^{\mathrm{T}}$, $\beta_{\mathrm{g}} = [0^{\mathrm{T}}\ (-M^{-1}P_{\mathrm{g}})^{\mathrm{T}}]^{\mathrm{T}}$ and $\beta_{\ell} = \left[P_{\ell}^{\mathrm{T}}\ Q_{\ell}^{\mathrm{T}}\right]^{\mathrm{T}}$, then we have

$$\begin{aligned} &\dot{x} = f(x,y) - \beta_{\mathrm{g}}, \\ &0 = g(x,y) - \beta_{\ell}, \end{aligned} \tag{2}$$

where

$$f(x,y) = \begin{bmatrix} \omega^{\mathrm{T}} & (-M^{-1}D\omega - M^{-1}f_{\mathrm{g}}(\delta_{\mathrm{g}}, \delta_{\ell}, V))^{\mathrm{T}} \end{bmatrix}^{\mathrm{T}},$$
$$f : \mathbb{R}^n \times \mathbb{R}^m \times \mathbb{R}^k \to \mathbb{R}^n$$

and

$$g(x,y) = \begin{bmatrix} f_{\ell}^{\mathrm{T}}(\delta_{\mathrm{g}}, \delta_{\ell}, V) & g_{\ell}^{\mathrm{T}}(\delta_{\mathrm{g}}, \delta_{\ell}, V) \end{bmatrix}^{\mathrm{T}},$$
$$g : \mathbb{R}^n \times \mathbb{R}^m \times \mathbb{R}^k \to \mathbb{R}^m \quad \text{are} \quad C^1.$$

It is well known that when parameters are subject to variations, the equilibria of the index-1 DAE of (2) may exhibit singularity induced (SI) bifurcation [3] as well as other frequently encountered local bifurcations such saddle node (SN) and Hopf bifurcations. With an SI bifurcation theorem ([3, Theorem 3, p. 1999]), an improved version of it based on the decomposition of parameter dependent polynomials can also be found in [4], Venkatasubramanian et al. have shown that the SI bifurcation occurs when system equilibria encounter the singularity manifold and it refers to a stability change owing to one eigenvalue of a reduced Jacobian matrix associated with the equilibrium diverging to infinity. Beardmore [5] has extended the SI bifurcation theorem of [3] to include non-generic cases whereby branching of equilibria is located at the singularity (i.e., the assumption 2 of the SI bifurcation theorem in [3] is lifted) and applied it to a 3-bus power system, which has been also studied by Kwatny et al. [1]. Riaza et al. [6] have provided a detailed study on the qualitative nature of singular points indicating that in some cases dynamic behavior of the system is smooth (well-defined vector field) even at singular points.

An important implication of the occurrence of the SI bifurcation is the existence of a singular set (or impasse surface) in the constraint manifold containing infinitely many singular points at each parameter value, which may play a crucial role in assessing the stability of DAE power system models. The literature in power system stability analysis with respect to the algebraic singularities of the DAEs is rich with references describing voltage instabilities in terms of the following: Eventual (or actual) loss of voltage causality, i.e., load bus variables (the algebraic variables) y cannot be described as a function of generator variables (the natural state variables) x [1], sudden change in voltages [7], nearness to an impasse surface [8,9], and loss of the small-signal stability in a real power system due to the occurrence of an SI bifurcation [10], to name a few. In [7], Hiskens et al. have shown that the existence of the impasse surface is closely related to the load models, and for constant load model the DAE model has the properties of voltage instability (i.e., sudden reduction in voltages) when operating in the vicinity of impasse points (or trajectories coinciding with the impasse surface). In [8,9], Loparo et al. have reported similar results and using the bifurcation theory they have shown that an important part of the stability boundary is formed by trajectories that are tangent to the singular surface. In

[10], Lerm et al. have studied local bifurcations in a real multi-parameter power system modeled as DAEs (South Brazilian power system) for which they have reported that stability region boundary of an operating point (i.e., an equilibrium point) contains SI bifurcations.

In spite of the fact that there is no well-established link between algebraic singularity and voltage collapse as in the case of the SN bifurcation, most of the work suggests that the system undergoes some sort of voltage instability when the voltage causality is lost during a transient. With respect to loss of voltage causality it is essential to note that during this, voltages are no longer implicit functions of dynamic variables when described by DAE models. To use DAE as a tool, knowledge of where causality disappears (or where impasse surface(s) "lie") can be applied towards the definition of "limits" of appropriateness for a given model. An underlying issue is that at singular points (including SI bifurcation points) the DAE model cannot predict the voltage behavior. Thus, location of singularities, which constitute important organizing elements of a power system DAE model, is invaluable information for assessing stability of the system. The family of singular points forms a boundary of well-defined behavior for a given model. In this work impasse surface is a set of singular points that exhibits loss of voltage causality.

Even though many researchers either in the field of electric power systems [1–3,7–10] or in the field of the general DAE theory [4–6] have long recognized the importance of singular points (or loss of voltage causality in power system applications) including SI bifurcation points in terms of system dynamics, there is no rigorous method available in the literature for computing their locations as a function of the system parameter. Most of the effort focuses on characterizing qualitative description of system dynamics around singularities without providing a systematic method to compute their locations in terms of system parameters, especially for large electric power systems. For relatively simple DAEs a convenient method to compute SI bifurcation points has been recently reported in [11] in which the DAE model is extended to an enlarged model by taking into account the SI bifurcation conditions. It has been shown that under some non-degeneracy conditions the SI bifurcation points of the original DAEs are associated with the regular equilibrium points (i.e., the point at which Jacobian matrix is non-singular) of the extended model. However, the implementation of this method is yet to be explored for the DAE models of electric power system.

This paper proposes a simple and efficient method to identify algebraic singularities (including SI bifurcation points) of the DAE model of power systems and to visualize singularities together with the equilibria and their associated local bifurcations as a function of the parameters using nose curves. In power system applications, nose curves are 2-dimensional (2-D) depiction of the evolution of the equilibria with respect to the changes in system parameters, and are usually used to show static stability margin of a current operating point in the parameter space. We bring the singular point information into the nose

curve and illustrate changes in both system equilibria and singular points as the parameter varies. This way of bringing information gathered from state space to parameter space gives a visual representation of the static and dynamic boundaries together in the same picture. The proposed method involves the following two main steps:

1. Computation of singular points at various parameter values along the nose curve defined by a designated bus injection (i.e., the system parameter) change pattern and illustrating singular points in the nose curve together with the equilibrium points.
2. Using the knowledge of location of singular points and exploiting the decoupled-parameter structure of DAE model of (2), identification of a new set of parameters and parameter increase pattern such that a selected singular points becomes an SI bifurcation point.

In the method for computing singular points, we first use generator angles to parameterize the algebraic part of the DAE model at any given parameter value (i.e., bus injections) and formulate the problem of identifying singular points as a bifurcation problem of a set of algebraic equations whose parameters are the generator angles. Then, at any given parameter value we implement an iterative technique that combines well-known Newton–Raphson (NR) and Newton–Raphson–Seydel (NRS) [12] methods to compute singular points as being SN bifurcations of load bus voltage magnitudes and angles in the constraint manifold. Finally, we exploit the decoupled-parameter structure of the DAE model of our interest to compute new set of parameters and parameter increase pattern such that any of the previously computed singular points become an SI bifurcation point.

2. Singularities of the DAE power system model

The general methods for studying the power system dynamics require the reduction of the DAE model of (2) to a locally equivalent set of ordinary differential equations (ODEs). However, this is possible only for the case when the algebraic variables (y) can be represented as functions of dynamic variables (x), which is known as voltage causality requirement [1]. In other words, at any causal point, say (x^*, y^*, β^*), the implicit function theorem ensures that there exists a function $\psi(x, \beta)$ defined on a neighborhood of (x^*, β^*) with $y^* = \psi(x^*, \beta^*)$ and that satisfies $g(x, \psi(x, \beta)) - \beta_\ell = 0$. It follows that trajectories of the DAE are locally defined by the ODEs:

$$\dot{x} = \phi(x, \beta) = f(x, \psi(x, \beta), \beta) \tag{3}$$

Typically, in a major part of the constraint manifold defined by

$$M(\beta) = \{(x,y) \in \Re^{n+m} | g(x,y) - \beta_\ell = 0, \beta = \text{constant}\} \tag{4}$$

such a reduction is possible and the ODEs uniquely define the dynamic behavior of DAEs. However, the constraint manifold will in general contain non-casual points (or singular points) at which equivalence is not possible. These singular points form a singular surface (or impasse surface) in the constraint manifold [3,7]. The singular surface is defined as

$$S(\beta) = \{(x,y) \in \Re^{n+m} | g(x,y) - \beta_\ell = 0;\ \det[D_y(g(x,y) - \beta_\ell)] = 0\}. \tag{5}$$

The SI bifurcation occurs when an equilibrium point, say (x_0, y_0) encounters the singularity of the algebraic equation, $g(x,y) - \beta_\ell = 0$ [3]. The SI bifurcation refers to stability change due to an eigenvalue of the reduced system matrix $[A_{\text{sys}}] = D_x\ f|_0 - D_y f|_0 [D_y g|_0]^{-1} D_y g|_0$ associated with the equilibrium point diverging to infinity from either $-\infty$ to $+\infty$, or vice versa. The set of SI bifurcation is defined as follows:

$$\text{SI}(\beta) = \left\{ (x,y,\beta) \in \Re^{n+m+k} \middle| \begin{matrix} f(x,y) - \beta_g = 0, \quad g(x,y) - \beta_\ell = 0 \\ \det[D_y(g(x,y) - \beta_\ell)] = 0 \end{matrix} \right\} \tag{6}$$

Remark 1. Note that since a singular $(x_s, y_s) \in S(\beta_s)$ at the parameter $\beta_s = [\beta_{sg}\ \beta_{s\ell}]^T$ is not an equilibrium point in general, there exists a non-zero parameter mismatch $\Delta\beta_{sg}$ representing real power mismatches at the generator buses, i.e., $\dot{x} = f(x_s, y_s) - \beta_{sg} = \Delta\beta_{sg} \neq 0$ while $g(x_s, y_s) - \beta_{s\ell} = 0$ and $\det[D_y(g(x_s, y_s) - \beta_{s\ell})] = 0$. Moreover, observe that the parameter β_g in (2) is decoupled from the rest of equation. This decoupled-parameter structure allows us to find a new set of parameters β_g^{new} such that a singular point (x_s, y_s) will be an SI bifurcation point (i.e., a singular equilibrium point) at this new parameter. In order to force a zero mismatch at the generator buses we can always define a new set of parameters $\beta_g^{\text{new}} = \beta_{sg} + \Delta\beta_{sg}$ such that

$$\begin{aligned} &\dot{x} = f(x_s, y_s) - \beta_g^{\text{new}} = 0, \\ &g(x_s, y_s) - \beta_{s\ell} = 0, \\ &\det[D_y(g(x_s, y_s) - \beta_{s\ell})] = 0. \end{aligned} \tag{7}$$

Therefore, a singular point $(x_s, y_s) \in S(\beta_s) = S(\beta^{\text{new}})$ at the parameter $\beta_s = [\beta_{sg}\ \beta_{s\ell}]^T$ is an SI bifurcation point at the new parameter $\beta^{\text{new}} = [\beta_g^{\text{new}}\ \beta_{s\ell}]^T$.

This remark indicates that we are able to identify the SI bifurcation points once singular points and the corresponding non-zero real power mismatch values at the singular points are available. In the following section we present an interative method to compute singular points at any given parameter value $\beta = [\beta_g\ \beta_\ell]^T$. The real power mismatches $\Delta\beta_{sg}$ can be easily computed by

evaluating differential equations at the singular point, i.e., $\Delta\beta_{sg} = f(x_s, y_s) - \beta_{sg}$.

3. Identification of singular points

In this section, we present an algorithm to compute singular points of DAE model of (2) at any given parameter value, β. The method is an iterative technique that combines well-known NR and NRS methods, which are commonly used to compute SN bifurcations of the equilibria in power systems [2]. The proposed algorithm benefits from the knowledge of the system equilibria and the occurrence of the SI bifurcation. Generator angles are parameterized through a scalar parameter in the constraint manifold. Then, at any given parameter value, the identification of a singular point is formulated as a bifurcation problem of a set of algebraic equations whose parameters are the generator angles. In the following, we explain why we parameterize generator angles and how this parameterization is achieved.

3.1. Parameterization of generator angles

Recall that the algebraic part of the DAE model of (2) represents the real and reactive power equations at the PQ load buses

$$0 = g(\delta_g, y) - \beta_\ell. \tag{8}$$

At a fixed parameter value, the constraint manifold consists of a set of points (δ_g, y) satisfying (8). The constraint manifold contains set of regular points at which the Jacobian matrix $[D_y(g(x,y) - \beta_\ell)]$ is non-singular and singular points. The set of regular points is known as voltage causal region in power system applications. The singular points lie on the boundary of the voltage causal regions. Fig. 1 hypothetically illustrates a magnified segment of the constraint manifold composed of two voltage causal regions, C_1 and C_2, and a singular point (δ_{gs}, y_s) connecting two regions. Note that the region C_1 contains an equilibrium point, upper equilibrium point, (δ_g^u, y^u) while the region C_2 contains another equilibrium point, lower equilibrium point (δ_g^ℓ, y^ℓ). These equilibria correspond to the high and low voltage equilibrium (or operating) points at a given parameter value β.

Observe that for any given generator angle δ_g there are two corresponding solutions for the algebraic variable y that represents the load bus voltage magnitude and phase angle. As the generator angle increases, these two solutions move along the regions C_1 and C_2 until they meet at the singular point (δ_{gs}, y_s). At the singular point, the Jacobian matrix $[D_y(g(x,y) - \beta_\ell)]$ becomes singular and there is no solution for y if δ_g is further increased. This observation indicates that algebraic variables meets at the singular point and they undergo an

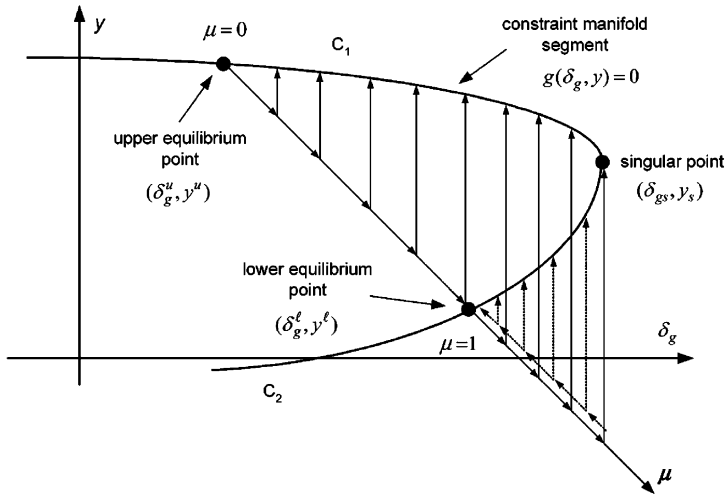

Fig. 1. Graphical illustration of the method for computing singular points.

SN bifurcation. This behavior is similar to the SN bifurcation of the equilibria as the bus injections change. This observation leads us to use generator angles as parameters and to seek methods to compute the SN bifurcations of algebraic varibles, which is a singular point of the DAE model.

In order to trace the corresponding segment of the manifold and to compute the singular point shown in Fig. 1 we need to implement an iterative method that initiates at a point in C_1 and ends up at another point in C_2 passing through the singular point (δ_{gs}, y_s). The upper and lower equilibrium points are the obvious choice for the starting and ending points of the algorithm since they are available to us from the equilibria computation. The following parameterization of the generator angles will achieve that purpose:

$$\delta_g = [(1-\mu)\delta_g^u + \mu\delta_g^\ell], \tag{9}$$

where δ^u and δ^ℓ are $(n-1)$-dimensional vectors representing the generator angles at the upper and lower equilibrium points at a given parameter value β, respectively, and μ is a new scalar bifurcation parameter.

With this parameterization, the identification of the singular point of the constraint manifold at a fixed parameter β reduces to a single parameter bifurcation problem of the following equation:

$$g(y, \mu) = 0. \tag{10}$$

Note that we drop the parameter β_ℓ in (10) for the sake of simplicity in the notation. Clearly, the SN bifurcation (i.e., branching) of the algebraic variables y as the bifurcation parameter μ changes will be a singular point of the constraint manifold at the corresponding parameter β. In the following section,

we describe a two-staged algorithm that implements the NR and NRS methods to locate the singular points.

3.2. A combined NR and NRS method

As we have explained in the previous section, a singular point of the DAE model at a given parameter is a static bifurcation point of the load bus voltage magnitude and phase angles when the generator angles are subject to vary. Thus, the problem of computing a singular point is equivalent to identification of the SN bifurcation of the algebraic equation (10) as the scalar parameter μ varies (thus, δ_g changes through (9)). Therefore, we seek a singular point (y, μ) in the constraint manifold such that $\operatorname{rank}[D_y(g(y,\mu) - \beta_\ell)] = m - 1$. In other words, the singular points must belong to the constraint manifold and the Jacobian matrix must have a simple eigenvalue at the origin. We can rewrite these conditions as follows:

$$g(y,\mu) = 0, \tag{11}$$

$$[D_y g(y,\mu)]v_y = 0, \tag{12}$$

$$\|v_y\|_2 - 1 = 0, \tag{13}$$

where $y \in \Re^m$ is the algebraic variables (load bus voltage magnitude and phase angles), $[D_y g(y,\mu)] \in \Re^{m\times m}$ is the Jacobian matrix of the algebraic equations, $v_y \in \Re^m$ is the right eigenvector corresponding to the zero eigenvalue of the Jacobian matrix, and $\mu \in \Re^1$ is the bifurcation parameter used to vary the generator angles. Observe that (13) assures that the eigenvector v_y is non-trivial. Eq. (12) together with Eq. (11) establishes the singularity of Jacobian matrix.

The conventional NR method is the most common iterative technique to compute the roots of non-linear algebraic equations. This method can be applied to (10) as follows:

$$[D_y g(y_i,\mu)]\Delta y = -g(y_i,\mu), \quad y_{i+1} = y_i + \Delta y \tag{14}$$

The above iterative scheme works well almost every point in the constraint manifold. However, it will fail to converge around a singular point since the Jacobian matrix is close to the singularity. The NRS method has been effectively used to compute static bifurcation of the equilibria in power systems [2]. In order to apply the NRS method to (11)–(13), a real eigenvalue (λ) of $[D_{yg}(y,\mu)]$ is introduced as an independent variable. That will make it possible to implement an iterative scheme that goes around the singular point:

$$\begin{aligned} h_1 &= g(y,\mu) = 0, \\ h_2 &= [D_y g(y,\mu) - \lambda I]v_y = 0, \\ h_3 &= \|v_y\|_2 - 1 = 0 \end{aligned} \tag{15}$$

There are a total of $(2m + 1)$ equations in (15) and the same number of unknown variables while λ is the independent variable. For a given λ, (15) can be solved for the unknowns $\hat{z} = [y\ v_y\ \mu]^{\mathrm{T}}$

$$[D_{\hat{z}}H(\hat{z}_i)]\Delta\hat{z} = -H(\hat{z}_i), \quad \hat{z}_{i+1} = \hat{z}_i + \Delta\hat{z}, \tag{16}$$

where $H = [h_1^{\mathrm{T}}\ h_2^{\mathrm{T}}\ h_3^{\mathrm{T}}]^{\mathrm{T}}$ and $[D_{\hat{z}}H(\hat{z})]$ is the corresponding extended Jacobian matrix of (15) that includes the second-order derivatives.

The NRS algorithm, like any other Newton-iterative method, needs a good initial condition, that is a point in the constraint manifold close enough to the singular point along with the smallest real eigenvalue of $[D_y g(y,\mu)]$ and the corresponding right eigenvector v_y. Otherwise, we may experience convergence problems. Therefore, we first use the NR method. The NR computations proceed starting at the upper equilibrium point ($\mu = 0$) along the constraint manifold until it fails to converge. The last successful NR data point is used to implement an inverse iteration method [13] for estimating the eigenvalue of $[D_y g(y,\mu)]$ nearest $\lambda = 0$, and the corresponding right eigenvector v_y. This data is then used to initiate an NRS procedure using (16) to compute around the singular point for values of $\lambda \in [-\varepsilon_1, \varepsilon_2]$ with $\varepsilon_1, \varepsilon_2 > 0$. The value $\lambda = 0$ is always included and data at the singular point is thereby obtained.

4. Computation of new bus injections change pattern in parameter space

In the DAE model of classical power systems with constant PQ load buses, the set of parameter $\beta = [\beta_{\mathrm{g}}\ \beta_\ell]^{\mathrm{T}}$ represents real/reactive power injections at the buses. For a network consisting of the n_{g} number of generators and n_{pq} number of PQ load buses, the β_{g} parameter vector is in the form of $\beta_{\mathrm{g}} = [0^{\mathrm{T}}\ (-M^{-1}\mathrm{P_g})^{\mathrm{T}}]^{\mathrm{T}}$ where $P_{\mathrm{g}} = [P_2 \ldots P_{n_{\mathrm{g}}}]^{\mathrm{T}}$ denotes net real power injections to the $n_{\mathrm{g}} - 1$ number of generators. The set of parameters $\beta_\ell = [P_\ell^{\mathrm{T}}\ Q_\ell^{\mathrm{T}}]^{\mathrm{T}}$ denotes the load demands at the n_{pq} number of load buses where $P_\ell = [P_{n_{\mathrm{g}}+1} \ldots P_{n_{\mathrm{g}}+n_{\mathrm{pq}}}]^{\mathrm{T}}$ and $Q_\ell = [Q_{n_{\mathrm{g}}+1} \ldots Q_{n_{\mathrm{g}}+n_{\mathrm{pq}}}]^{\mathrm{T}}$ are the real and reactive power demands, respectively. Local bifurcation analyses of power systems identify qualitative changes in system equilibria, such as number of equilibria and their small-signal stability features as the bus injections are subject to vary. Changes in bus injections are achieved through parameterization of bus injections with a scalar parameter known as a bifurcation parameter

$$\beta = \beta^0 + \alpha * \ direction\,\beta \tag{17}$$

where β^0 is the base case bus injections, α is the scalar bifurcation parameter and $direction\,\beta = \begin{bmatrix} d_{P_{\mathrm{g}}}^{\mathrm{T}} & d_{P_\ell}^{\mathrm{T}} & d_{Q_\ell}^{\mathrm{T}} \end{bmatrix}^{\mathrm{T}}$ is the direction vector in the parameter space, which allows us to vary bus injections at a single bus and/or group of buses. The elements of *direction* β are given below:

$$d_{P_g} = \begin{bmatrix} d_{P_2} & \dots & d_{P_{n_g}} \end{bmatrix}^T; \quad d_{P_\ell} = \begin{bmatrix} d_{P_{n_g+1}} & \dots & d_{P_{n_g+n_{pq}}} \end{bmatrix}^T;$$
$$d_{Q_\ell} = \begin{bmatrix} d_{Q_{n_g+1}} & \dots & d_{Q_{n_g+n_{pq}}} \end{bmatrix}^T. \tag{18}$$

In power system applications, the evolution of system equilibria as the bifurcation parameter α varies is usually illustrated through the (2-D) equilibrium surfaces known as nose curves. Fig. 2 shows two nose curves each representing a different bus injection increase pattern defined by *direction* β^0 and *direction* β^{new}. Note that along the nose curve of *direction* β^0 two local bifurcations of equilibria, SI and SN bifurcations are illustrated. Of interest is the SI bifurcation that is said to have occurred when an equilibrium point meets a singular point associated with a bus injection increase pattern, say *direction* β^0. Note that various singular points along the nose curve are denoted by (x).

By Remark 1 given in the previous section, we show that any of these singular points could become an SI bifurcation point. For any of these singular points it is of our interest to determine a new bus injection change pattern, say *direction* β^{new}, such that the corresponding nose curve pass through the singular point as depicted in Fig. 2 by the nose curve of *direction* β^{new} indicating the occurrence of an SI bifurcation.

Remark 2. If we have a singular point (x_s, y_s) computed at $\alpha = \alpha_s$ for a designated bus injection change pattern defined by *direction* β^0 and the

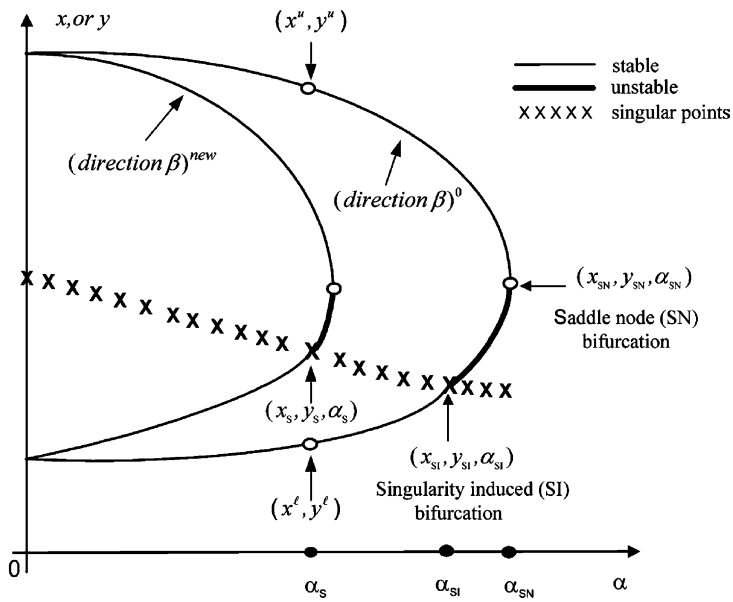

Fig. 2. Illustration of bifurcations of system equilibria and singular points in a 2-D nose curve.

corresponding non-zero real power mismatches at the generator buses ΔP_{sg}; a new bus injection change pattern defined by *direction* β^{new} that will cause the resulting nose curve to pass through this singular point at $\alpha = \alpha_s$ (i.e. an SI bifurcation) can easily be obtained. From (17) and (18), it is obvious that generator bus injections associated with *direction* β^0 at the singular point (x_s, y_s) are given by

$$P_{sg} = P_g^0 + \alpha_s d_{P_g}^0. \tag{19}$$

By the Remark 1, the new generator bus injections such that this singular point becomes an SI bifurcation point will be

$$P_g^{new} = P_g^0 + \alpha_s d_{P_g}^0 + \Delta P_{sg}. \tag{20}$$

By (17), this new injection can be achieved by

$$P_g^{new} = P_g^0 + \alpha_s d_{P_g}^{new}. \tag{21}$$

From (20) and (21) the new search direction corresponding to the generator buses will be

$$d_{P_g}^{new} = d_{P_g}^0 + \frac{1}{\alpha_s}\Delta P_{sg}. \tag{22}$$

Note that it is clear that components of the new direction vector corresponding to the PQ load buses (i.e., d_{P_ℓ} and d_{Q_ℓ}) will not change: $d_{P_\ell}^{new} = d_{P_\ell}^0$; $d_{Q_\ell}^{new} = d_{Q_\ell}^0$.

5. Simulation results

In this section, we present the application of the method for computing singular points and SI bifurcations presented in the previous sections to a 5-bus power system with three generators and two constant PQ load buses [8], whose one-line diagram is illustrated in Fig. 3. The base case bus injections in per unit (pu) with a 100 MW base are as follows:

$$P_g^0 = [P_2 \quad P_3]^T = [5 \quad 5]^T; \quad P_\ell^0 = [P_4 \quad P_5]^T = [-10 \quad -5]^T \quad \text{and}$$
$$Q_\ell^0 = [Q_4 \quad Q_5]^T = [-3 \quad -2]^T \text{ pu}$$

Generators, which are undamped with unity inertia, have the internal voltages $E = [1.2\ 1.2\ 1.2]^T$ pu that are equal to terminal voltages since the reactance $x_d = 0.1$ pu includes the transient reactances of the generator and transmission line. The generator 1 is chosen as the swing bus with zero angle and all the other phase angles are relative to the swing bus.

In order to determine a set of equilibrium points we vary mechanical inputs to the generators 2 and 3 (P_2 and P_3); and real/reactive power demand at bus 4

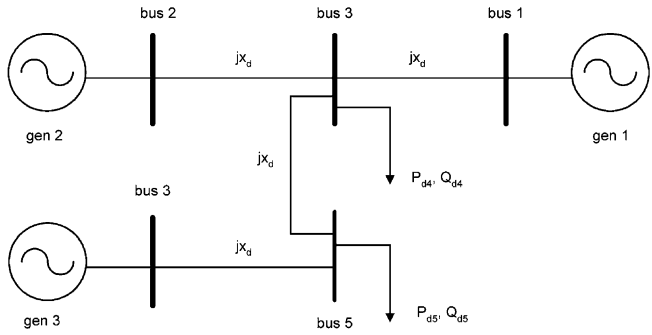

Fig. 3. One-line diagram of the 5-bus electric power system.

while the power factor is kept constant at this bus. The resulting search direction in the bus injection space is as follows: $d^0_{P_g} = [0.5\ 0.5]^T$; $d^0_{P_\ell} = [-0.5\ 0]^T$; $d^0_{Q_\ell} = [-0.15\ 0]^T$. Note that entries of $d^0_{P_g}$ are set be positive, which indicates increase in generators' mechanical power input and those of $d^0_{P_\ell}$ and $d^0_{Q_\ell}$ are set to be negative (or zero for the bus 5), which indicates increase in real/reactive power demand at the PQ load bus 4.

Fig. 4 illustrates how the equilibria for the voltage magnitude at bus 4 (V_4) and their corresponding small-signal stability characteristics change with parameter variations. Observe that as the parameter α varies the system equilibria undergo SN and SI bifurcations labeled as SN and SI (S_1), respectively. As the bus injections are increased through the scalar parameter α both high

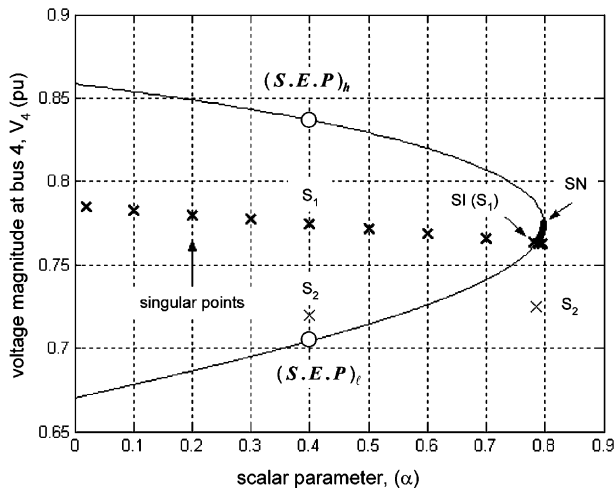

Fig. 4. Voltage magnitude at bus 4 (V_4) and singular points vs. parameter alpha (α) for *direction* β^0.

voltage equilibrium $(SEP)_h$ and low voltage equilibrium $(SEP)_l$ points are dynamically stable. However, at $\alpha_{SI} = 0.785$ the low voltage equilibrium point undergoes a stability exchange (stable → unstable) due to an SI bifurcation and it becomes a type-1 unstable equilibrium point. Further increase in the parameter α causes the high and low voltage equilibria meet at an SN bifurcation for $\alpha_{SN} = 0.8$.

The SN and SI bifurcations are detected by monitoring the eigenvalues of system matrix as the system moves from one equilibrium point to another with changes in the bifurcation parameters α. Fig. 5 shows how two critical eigenvalues of the system matrix moves as α changes from $\alpha = 0.773$ to $\alpha = 0.8$ along the lower branch of nose curve; which leads to SI and SN bifurcations. The arrows indicate the direction of increase in the parameter α. Just before the SI bifurcation; say at $\alpha = 0.773$, the critical eigenvalues (please note that non-critical ones are not shown in Fig. 5) are located in the left half plane, which implies stability. As the parameter changes from $\alpha = 0.783$ to $\alpha_{SI} = 0.785$ one of the complex eigenvalue moves (in a jump fashion) to the right half plane and becomes a large positive number while the other eigenvalue stays in the left half plane but it becomes a large negative real number. Therefore, stability feature of the equilibria undergoes an instantaneous change from stable to unstable with exactly one eigenvalue. This stability exchange is due to an SI bifurcation at which the Jacobian matrix $[D_y\, g(x,y)]$ has a simple eigenvalue at the origin and one of the eigenvalues of system matrix $[A_{sys}]$ becomes unbounded [3]. A clear picture of the occurrence of the SI bifurcation with a much larger real

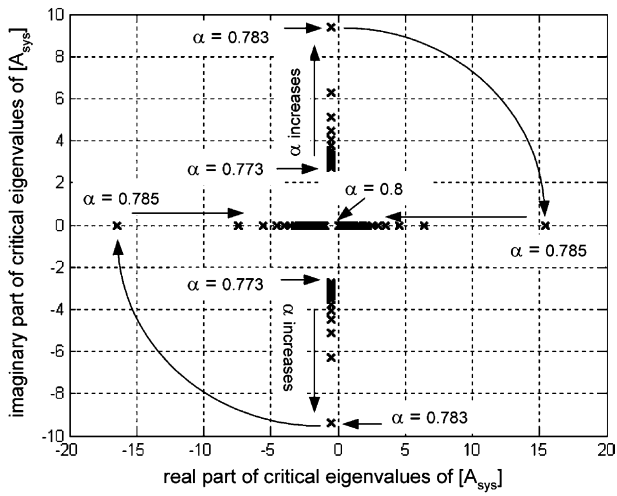

Fig. 5. Critical eigenvalues of the system matrix $[A_{sys}]$ as the parameter alpha (α) varies indicating the SI and SN bifurcations.

eigenvalue can be obtained at the expense of simulation time [14]. As α increases further an SN bifurcation occurs at $\alpha_{SN} = 0.8$ and one of the critical eigenvalues of $[A_{sys}]$ becomes zero while the other one remains in the left half plane.

Fig. 4 also shows singular points computed at various values of α along the nose curve, which are depicted by (x) and labeled as S_1. It is worth mentioning here that there are multiple singular points at any given parameter α. However, we are interested in those that eventually meet with one of the equilibria located in the lower branch of the nose curve as the parameter α is subject to vary as illustrated in Fig. 4. Note that the singular point S_1 at $\alpha_{SI} = 0.785$ coincides with low voltage equilibrium indicating an SI bifurcation. In Fig. 4, we also depict another singular point (S_2) for $\alpha = 0.4$ and $\alpha_{SI} = 0.785$ as to clearly show the relative locations of other singular points that are not associated with the SI bifurcation.

The relative location of singular points with respect to equilibria and SI bifurcation point can be clearly seen using 2-D projections of the constraint manifold. Fig. 6 shows a 2-D projection of the constraint manifold onto the (V_4, δ_2)-space for $\alpha = 0.4$. The constraint manifold consists of two voltage causal regions (C_1 and C_2) separated by singular points S_1 and S_2. Note that each voltage causal region contains a dynamically stable equilibrium points labeled as $(SEP)_h$ and $(SEP)_l$. These equilibrium points correspond to high and low voltage equilibrium points at $\alpha = 0.4$ shown in Fig. 4. Singular points S_1 and S_2 are the same ones shown in Fig. 4 at $\alpha = 0.4$, and they indicate the branching of the algebraic variables (i.e., load bus voltage magnitudes and angles) when generator angles are considered as parameters. It will be informative to

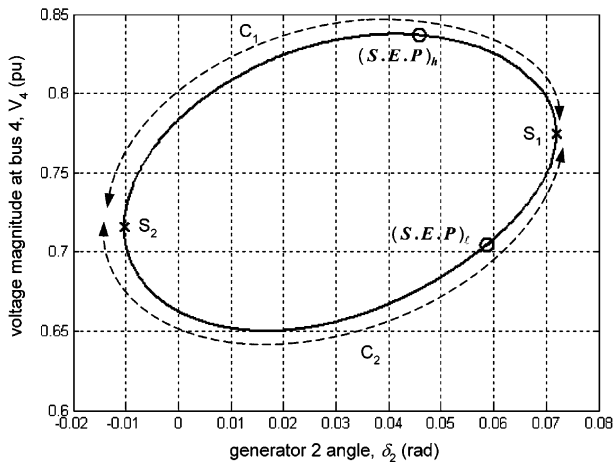

Fig. 6. Constraint manifold projection onto the (V_4, δ_2)-space at $\alpha = 0.4$ for *direction* β^0.

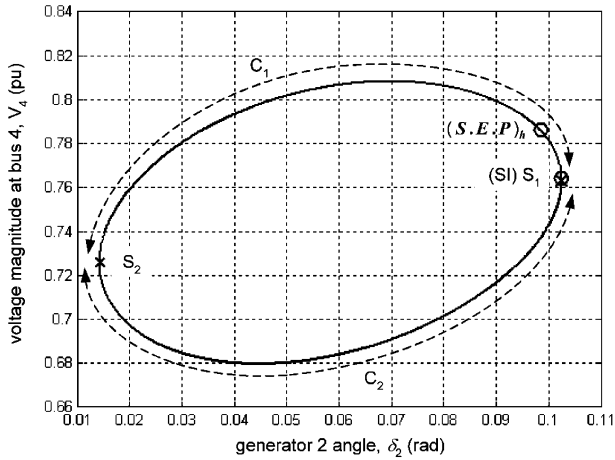

Fig. 7. Constraint manifold projection onto the (V_4, δ_2)-space at $\alpha = 0.785$ for *direction* β^0.

illustrate the occurrence of the SI bifurcation by using the constraint manifold projection. Fig. 7 shows the same 2-D projection onto the (V_4, δ_2)-space for $\alpha_{SI} = 0.785$. This time; however, the low voltage equilibrium point $(SEP)_l$ moves along the region C_2 as α increases from $\alpha = 0.4$ to $\alpha_{SI} = 0.785$ and coincides with the singular point S_1 while the high voltage one, $(SEP)_h$, stays in the region C_1. Note that for this load increase pattern, both equilibria move toward the singular point S_1 not toward S_2 along the regions as the parameter α varies. Therefore, S_2 or any other singular points rather than S_1 are not associated with the SI bifurcation.

As indicated in Remarks 1 and 2, any of the singular points shown in Fig. 4 along the nose curve could become an SI bifurcation point; and a new search direction such that resulting nose curve passes through this SI bifurcation point could easily be determined. In the following, we illustrate these steps for $\alpha = 0.4$: The real power mismatch vector at $\alpha = 0.4$ is found as $\Delta P_g = [\Delta P_2 \ \Delta P_3]^T = [-0.085 \ 03413]^T$. Following (22), entries of the new search direction corresponding to generator buses 2 and 3 will be $d_{P_g}^{new} = \begin{bmatrix} d_{P_2}^{new} & d_{P_3}^{new} \end{bmatrix}^T = \begin{bmatrix} 0.2875 & 1.3533 \end{bmatrix}^T$. Note that entries of the search direction vector corresponding to the PQ load buses (i.e., buses 4 and 5) will not change: $d_{P_\ell}^{new} = d_{P_\ell}^0 = \begin{bmatrix} -0.5 & 0 \end{bmatrix}^T$ and $d_{Q_\ell}^{new} = d_{Q_\ell}^0 = \begin{bmatrix} -0.15 & 0 \end{bmatrix}^T$. The resulting search direction vector that will yield a set of new equilibria including the singular point S_1 at $\alpha = 0.4$ as being an SI bifurcation point is computed as

$$direction\ \beta^{new} = \begin{bmatrix} 0.2875 & 1.3533 & -0.5 & 0 & -0.15 & 0 \end{bmatrix}^T.$$

The above procedure can easily be repeated for other singular points along the nose curve. Fig. 8 illustrates three more nose curves obtained by new search

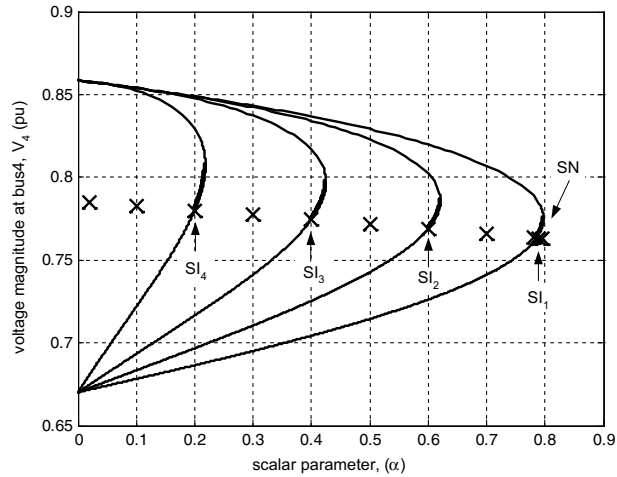

Fig. 8. Collection of nose curves indicating singularity induced bifurcations.

directions at parameters $\alpha = 0.2, 0.4$, and 0.6 together with original nose curve shown in Fig. 4. Note that each of new nose curves passes thru a singular point, which is an SI bifurcation point. These new SI bifurcation points are labeled as SI_2, SI_3, and SI_4.

Fig. 9 illustrates the stability region in the generator injection space (P_{g2}, P_{g3}-space) whose boundary is determined by the SI bifurcation depicted

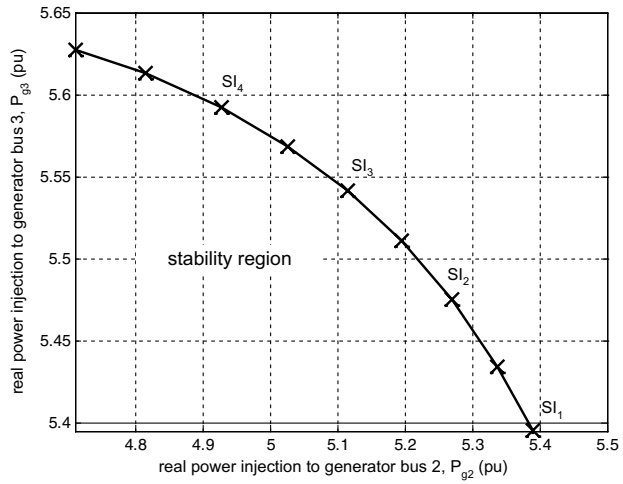

Fig. 9. SI bifurcation boundary in the generator injection space for a given load increase scenario specified by the direction vectors $d_{P_\ell} = [-0.5\ 0]^T$ and $d_{P_\ell} = [-0.15\ 0]^T$ for the load buses.

in Fig. 8. The region shows the possible set of generator injections that avoids the occurrence of SI bifurcation for given load increase pattern specified by the direction vectors $d_{P_\ell} = [-0.5\ 0]^T$ and $d_{Q_\ell} = [-0.15\ 0]^T$ for the load buses (buses # 4 and 5).

6. Conclusions

In this paper we have presented an iterative method to locate and identify singular points of the DAE model of the classical power system with constant PQ load buses. In the method, generator angles are used to parameterize the algebraic part of the DAE model and singular points are computed as being the SN bifurcation of the algebraic part of the DAE model using a combined NR–NRS iterative algorithm. Based on knowledge of location of singular points and exploiting the decoupled structure of the DAE model we have determined new search directions in the bus injection (parameter) space. It has been shown that set of equilibrium point corresponding to the new search directions undergoes an SI bifurcation at the low voltage portion of the nose curve. The simulation results for a 5-bus electric power system indicate the effectiveness of the method.

The depiction of singular points together with the equilibria and their corresponding local bifurcations as a function of the parameters provides a comprehensive picture of the stability of the DAE model. Moreover, to use DAE as tool for the analysis of power system dynamics, knowledge of where singular points are located and how their location are changed with respect to parameters can be applied towards the definition of "limits" of appropriateness for a given model.

Acknowledgement

This work was supported in part by the US Department of Energy under Contract # ER63384.

References

[1] H.G. Kwatny, A.K. Pasrija, L.Y. Bahar, Static bifurcations in electric power networks: Loss of steady state stability and voltage collapse, IEEE Trans. Circuits Syst. I 33 (10) (1986) 981–991.

[2] H.G. Kwatny, R. Fischl, C.O. Nwankpa, Local bifurcation in power systems: Theory, computation, and application, Proc. IEEE 83 (11) (1995) 1456–1483.

[3] V. Venkatasubramanian, H. Schättler, J. Zaborszky, Local bifurcations and feasibility regions in differential-algebraic systems, IEEE Trans. Automat. Contr. 40 (12) (1995) 1992–2013.

[4] L. Yang, Y. Tang, An improved version of the singularity-induced bifurcation theorem, IEEE Trans. Automat. Contr. 46 (9) (2001) 1483–1486.

[5] R.E. Beardmore, Stability and bifurcation properties of index-1 DAEs, Numer. Algorithms 19 (1998) 43–53.
[6] R. Riaza, S.L. Campell, W. Marszalek, On singular equilibria of index-1 DAEs, Circuits Syst. Signal Process 19 (2) (2000) 131–157.
[7] I.A. Hiskens, D.J. Hill, Energy function, transient stability and voltage behavior in power systems with nonlinear loads, IEEE Transact. Power Syst. 4 (1989) 1525–1533.
[8] K.L. Praprost, K.A. Loparo, An energy function method for determining voltage collapse during a power system transient, IEEE Trans. Circuits Syst. I 41 (10) (1994) 635–651.
[9] K.L. Praprost, K.A. Loparo, A stability theory for constrained dynamic systems with applications to electric power systems, IEEE Trans. Automat. Contr. 41 (11) (1996) 1605–1617.
[10] A.P. Lerm, C.A. Cañizares, A.S. Silva, Multi-parameter bifurcation analysis of the South Brazilian power system, IEEE Trans. Power Syst. 18 (2) (2003) 737–746.
[11] K.H. Yasir, Y. Tang, Computation of the singularity induced bifurcation points in DAEs via extended system reduction, Appl. Numer. Math. 44 (2003) 425–431.
[12] R. Seydel, Practical Bifurcation and Stability Analysis—from Equilibrium to Chaos, Springer-Verlag, New York, 1994.
[13] R.L. Burden, J.D. Faires, Numerical Analysis, 6th ed., Brooks/Cole, 1997.
[14] Ayasun S, Nwankpa CO, Kwatny HG, Numerical issues in the location of singularity induced bifurcation points. In: Proceedings of the IEEE PES Winter Meeting, New York City, New York; February 1999. p. 707–712.